Biomaterials Science

ROYAL SOCIETY OF CHEMISTRY

PAPER

View Article Online
View Journal | View Issue

Cite this: *Biomater. Sci.*, 2025, **13**, 6038

Mucin 1 antigen mimetic functionalized mannosylated peptide nanofibers for antigen uptake and immune modulation

Silvia Fallarini,[a] Andrea Sodini,[b] Filippo Susini,[b] Gaia Lesca,[a] Silvia Scaglione,[c] Maria Elisabetta F. Palamà,[c] Francesca Maestrelli,[b] Maria Cristina Salvatici,[d] Federica Cefalì,[b] Mustafa O. Guler,[e]* Ayse Begum Tekinay[f]*† and Cristina Nativi[b]*

Received 26th February 2025,
Accepted 18th August 2025

DOI: 10.1039/d5bm00304k

rsc.li/biomaterials-science

In this work, immune modulation of monocyte-derived dendritic cells was studied using *in vitro* cell culture and organ-on-chip models. Self-assembled mannosylated peptide nanofibers were prepared and integrated with the MUC1 TnThr mimetic **Tn-MIM**, to stimulate DCs' maturation and differentiation. The nanofibers obtained (namely Man-PA/**Tn-MIM**) showed remarkable cell-penetrating capabilities and allowed the correct presentation of the antigen mimetic with a corresponding induction of lymphocyte, iNKT and NK cell recruitment. The Man-PA/**Tn-MIM** integrated nanofibers were also found to direct the immune response towards the Th1 phenotype, which is responsible for the production of cellular and humoral immunity. Organ-on-chip tests confirmed the cytotoxicity of lymphocytes stimulated with DCs exposed to Man-PA/**Tn-MIM**. These results will help in the development of immunotherapies avoiding complications due to heterogeneous antigen presentation and the use of adjuvants.

Introduction

Mucosal tissues expose a large surface area to the external environment and come into contact with viruses, bacteria, yeast, and parasites that cause human diseases. The mucosal epithelial cells shield the host from these harmful species forming a physical barrier and secreting defensive compounds, especially mucins.[1] Epithelial mucins are a family of complex glycoproteins characterized by branched *O*-glycosides densely decorating large peptide domains of repeating amino acid sequences, rich in serine (Ser), threonine (Thr), and proline (Pro).[1]

It has previously been observed that mucins' glycosylation patterns change in response to mucosal infection and inflammation. For instance, epithelial tumor cells overexpress mucin 1 (MUC1) glycoprotein featuring aberrant oversimplified, truncated oligosaccharides.[2] Therefore, saccharide determinants such as the monosaccharide Tn (α-*O*-GalNAc linked to a residue of Ser or Thr) (see Fig. 1) normally hidden by extensive *O*-glycosylation, in tumors become exposed to the immune system. Therefore, it is expected that tumoral MUC1 fragments (*i.e.* Tn-glycosylated PDTR, GSTA, and GVTS or analogues) serve as targets for cancer immunotherapy.[2–7] However, MUC1 glycopeptides are poorly immunogenic and tolerated by the immune system, which is not efficiently activated against tumors. To break this tolerance and amplify the immunogeni-

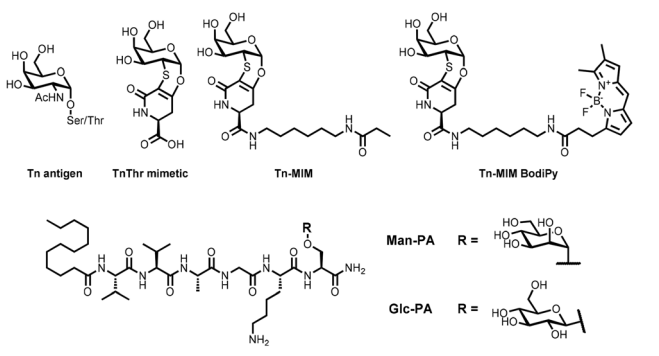

Fig. 1 Structure of the native Tn antigen, TnThr mimetic, alkyl derivative of the TnThr mimetic (**Tn-MIM**), and fluorescent TnThr mimetic (**Tn-MIM** BodyPy) and chemical structure of self-assembling peptide amphiphile molecules (Man-PA and Glc-PA).

[a]*University of Piemonte Orientale, Department of Pharmaceutical Sciences, Largo Donegani 2, Novara 28100, Italy*
[b]*Department of Chemistry, DICUS, University of Florence, via della Lastruccia, 3-13, 50019 Sesto F.no, Italy. E-mail: cristina.nativiU+0040unifi.it*
[c]*React4Life S.p.A., Via Greto di Cornigliano, 6/R, 16152 Genova, Italy*
[d]*Institute for the Chemistry of Organometallic Compounds (CNR-ICCOM), via Madonna del Piano10, 50019 Sesto F.no, Italy*
[e]*The Pritzker School of Molecular Engineering, The University of Chicago, 5640 S Ellis Ave, Chicago, IL 60637, USA. E-mail: Mguler@uchicago.edu*
[f]*Requalite GmbH, Hans-Cornelius-Straße 4, 82166 Gräfelfing, Germany*
† Present address: Ttech Biotechnology, Alinteri Blv., 1151. Sk., No:1, Ostim OSB, Ankara, Turkiye.

city of these constructs, carrier proteins (like KLH, OVA, or CRM197) have been used.[8] Yet, immunogenic carriers eliciting non-specific immune responses trigger side effects and dampen the specific anti-glycopeptide antibody response. Even though interesting alternatives have been proposed,[6,9–14] chemically defined candidates able to induce an effective immune response without an external adjuvant are yet to be developed.

We and others demonstrated the use of peptide nanofibers as antigen delivery agents for nano-vaccine candidates.[15–17] Peptide nanofibers are biocompatible and biodegradable materials[18] formed by self-assembling peptide amphiphiles (PAs); however, unlike more conventional delivery vesicles, PAs can be functionalized with targeting molecules/antigens. The antigens delivered through nanoscale materials are considerably advantageous over soluble antigen administration thanks to cellular activation by surface-functionalized delivery vectors. Notably, tailored peptide nanofibers have been reported to present a variety of functional groups or residues to successfully target specific cells.[19] In addition, the high capacity of peptide nanofibers to amplify the uptake of antigens by Antigen Presenting Cells (APCs) and enhance immune responses has been demonstrated.[20,21]

Dendritic Cells (DCs) are APCs' essential targets for immunotherapy and vaccination approaches. DCs can coordinate innate and adaptive immune responses by capturing, processing, and presenting antigens to T-cells. T-cells activated by a tumor antigen presented by DCs trigger anticancer responses.

We previously showed that properly functionalized self-assembling mannosylated glycopeptide nanofibers not only induced remarkable DC activation but also demonstrated their potential to be employed as adjuvants.[20] Here, self-adjuvating glycopeptide nanofibers were used for the presentation and delivery of the mimetic of the MUC1 TnThr epitope (namely the TnThr mimetic; see Fig. 1). The TnThr mimetic is an effective antigen mimetic able to induce a specific immune response in a triple-negative breast cancer (TNBC) animal model[22] and to efficiently intercept naturally occurring tumor-associated autoantibodies against MUC1 in human serum.[6] In this work, self-assembled mannosylated peptide nanofibers were used to present and deliver multiple copies of the TnThr mimetic, effectively promoting dendritic cell (DC) activation and maturation, as well as inducing allostimulation and T-helper (Th) cell polarization. The immunomodulation properties of the glycopeptide nanofibers were further confirmed by using an organ-on-chip breast cancer model.

Results and discussion

Preparation of self-adjuvating glycopeptide nanofibers Man-PA and Glc-PA

Following a previously reported protocol,[20] glycosylated serine residues Fmoc-L-Ser[α-D-Man(OAc)$_4$]-OH and Fmoc-L-Ser[β-D-Glc(OAc)$_4$]-OH were first synthesized (see the SI) prior to the synthesis of respectively Man-PA and Glc-PA. The peptide synthesis was accomplished by a solid phase peptide synthesis method. After the resin cleavage, the amphiphilic glycopeptides were obtained in protected form. Then, the acetyl protecting groups of sugar hydroxyls were removed in solution (see the SI for details). Despite the presence of a glycosylated amino acid residue at the peptide C-terminus, the amphiphilic character of the glycopeptides was obtained by the conjugation of a hydrocarbon tail to the N-terminus (see Fig. 1). The mannose residue was chosen for its high affinity to the DC-SIGN receptor and consequent induction of DC activation. The glucose residue was selected as a negative control to investigate the sugar specificity of glycosylated PA scaffolds.[23]

Synthesis of the alkylated TnThr mimetic (Tn-MIM) and fluorescent Tn-MIM (Tn-MIM BodiPy)

To integrate the TnThr mimetic into glycopeptide systems, the alkylated derivative **Tn-MIM** was synthesized (Scheme 1). **Tn-MIM** was prepared in one step and in good yield (75%) from compound **1** [22] upon reaction with propanoic acid, *O*-(benzotriazol-1-yl)-1,1,3,3-tetramethyluronium tetrafluoroborate (TBTU) and *N*-methyl morpholine-*N*-oxide (NMM) at room temperature, in DMF as solvent. For cell internalization analyses, a BodiPy-tagged derivative of **Tn-MIM** was synthesized. Thus, **Tn-MIM** BodiPy was obtained by treating a solution of **1** in DMF–H_2O and sodium bicarbonate with BodiPy derivative **2** at 0 °C. After 12 h at room temperature, the reaction was completed, and the desired compound was isolated in good yield (60%; see the SI) (Scheme 1).

Tn-MIM integrated glycopeptide nanofibers

The integration of the poor water-soluble **Tn-MIM** into the glycopeptide nanofibers was accomplished by a solvent exchange technique. A biphasic solution was prepared by treating the selected glycopeptide dissolved in slightly acid water and sonicated (pH 6, 40 °C) with a solution of **Tn-MIM** in a DCM : MeOH (7 : 1, v/v) mixture (see the SI for details).[20] The biphasic solution was heated and sonicated to allow the hydrophobic tail region of **Tn-MIM** to self-organize with the hydro-

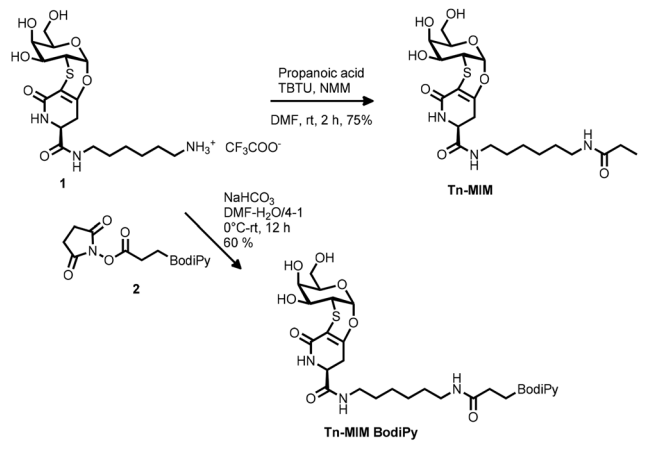

Scheme 1 Synthesis of **Tn-MIM** and **Tn-MIM** BodiPy.

phobic tail of the glycopeptide, promoting the **Tn-MIM** phase transfer. **Tn-MIM** integrated Glc-PA (Glc-PA/**Tn-MIM**) and **Tn-MIM** integrated Man-PA (Man-PA/**Tn-MIM**) were thus prepared.

To highlight the integration of **Tn-MIM** into the glycopeptide nanofibers, BodiPy-tagged **Tn-MIM** was prepared (see Scheme 1) and integrated into Man-PA (Fig. 2). After solvent exchange (Fig. 2C), the fluorescent **Tn-MIM** was no longer observed in DCM. Spectroscopic analyses confirmed the transfer of the alkylated mimetic into the water phase (see the SI for details).

Characterization of the nanofibers

Before the integration of **Tn-MIM** or **Tn-MIM**-BodiPy into the glycopeptide systems, the amphiphilic glycopeptides (Man-PA and Glc-PA) were studied in terms of their secondary structure and morphological features at physiological pH. Circular Dichroism (CD) of Man-PA or Glc-PA solutions (H_2O, 200μM) showed that both pure systems were organized in a β-sheet conformation (see Fig. S1). Morphological studies carried out by using transmission electron microscopy (TEM) showed that both glycopeptide samples form high-aspect-ratio nanofibers (diameters on the order of 15–25 nm and lengths reaching several micrometers; see Fig. S2), regardless of the type of monosaccharide they contain (Fig. 3).

DC viability assay and iDC differentiation

To investigate the ability of glycosylated nanofibers to induce DC maturation and differentiation, an *in vitro* monocyte-derived dendritic cell (mo-DC) model was used. Monocytes from healthy volunteer buffy coats were differentiated into immature DCs (iDCs; see the SI for details) to efficiently present antigens to professional APCs like DCs. The evaluation by flow cytometry of cytokine-treated monocytes proved a reduction of CD14 and an increase of HLA-DR, confirming the generation of iDCs (Fig. 4B).

Cytotoxicity is a key factor when designing materials for delivery; thus, nanofibers' cytotoxic potential was evaluated before running morphological and functional assays. iDCs were thus treated for 48 h with increasing concentrations (0.1–10 μM; see the SI for details) of **Tn-MIM**, Man-PA, Glc-PA, Man-PA/**Tn-MIM** and Glc-PA/**Tn-MIM**. No reduction in iDC viability was observed at all concentrations tested (data not shown), so all compounds were screened in the following experiments.

iDCs, through the interaction with harmful species or inflammatory stimuli like cytokines or cell debris, can become mature, upregulating HLA-DR and co-stimulatory molecules to efficiently induce T cell activation. Accordingly, the compounds' ability to induce maturation was evaluated and iDCs were treated (48 h) with increasing concentrations (0.1–10 μM) of each compound. CD40, CD80 and HLA-DR expression increased on iDCs treated with Man-PA and, to a higher extent, on iDC treated with Man-PA/**Tn-MIM**. CD86 expression also significantly increased upon treatment with Man-PA/**Tn-MIM** (Fig. 4 and Table S1). These results demonstrate that Man-PA possesses an intrinsic stimulatory activity that is enhanced by **Tn-MIM** internalization. The sugar specificity of the glycosylated PA scaffolds is in line with the high affinity of DC-SIGN for mannosyl-containing glyco-constructs;[24] in fact, Man-PA

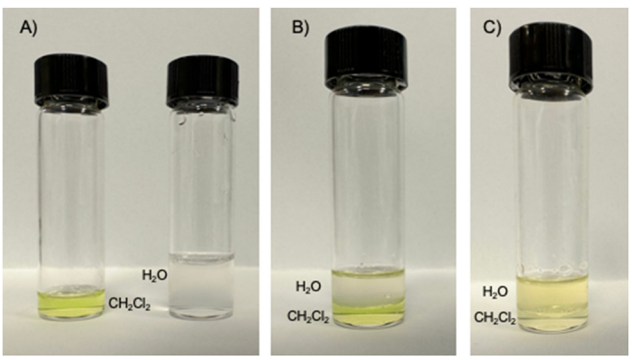

Fig. 2 Image of DCM–H_2O solvent exchange for **Tn-MIM**-BodiPy. (A) Vial with **Tn-MIM** BodiPy dissolved in CH_2Cl_2 and vial with H_2O; (B) before solvent exchange; (C) after solvent exchange.

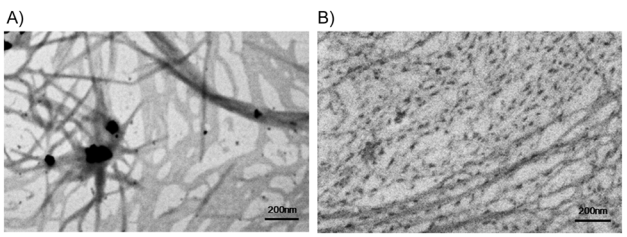

Fig. 3 TEM images of Man-PA/**Tn-MIM** (A) and Glc-PA/**Tn-MIM** (B).

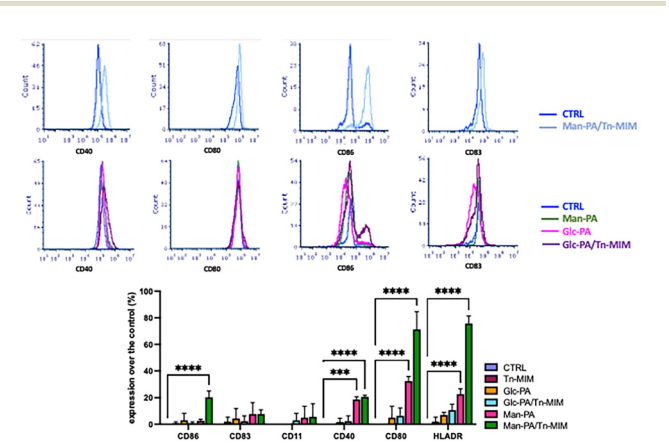

Fig. 4 Expression of activated receptors on moDC after treatment with tested compounds. iDCs treated (48 h) with **Tn-MIM**, Man-PA, Glc-PA, Glc-PA/**Tn-MIM** and Man-PA/**Tn-MIM** (10 μM) were harvested, washed, and stained with specific antibodies and the MFI of each marker was evaluated by FACS. (A) Representative histograms of some markers expressed by iDC treated with Man-PA (green line), Glc-PA (pink line), Glc-PA/**Tn-MIM** (purple line) and Man-PA/**Tn-MIM** (light blue line) (10 μM); (B) fold increase over the control of the marker MFI. The results represent the mean ± SEM of at least three experiments conducted with iDCs obtained using different donors. See the SI for endotoxin contamination control.

itself has more stimulation ability than Glc-PA or Glc-PA/**Tn-MIM**. The differentiation of iDCs to mature phenotypes able to stimulate T cell responses was thus obtained. Notably, the **Tn-MIM** molecule itself did not induce any iDC maturation, indicating that the loading on Man-PA is a requisite for the maturation of iDCs. Based on the observed increases upon treatment of iDCs with 10 μM of each compound, this concentration was selected for the subsequent experiments.

To get insights into iDC maturation induced by glycosyl peptides, we evaluated the TNF-α and IL-12 levels released by DCs in the cell culture medium.

TNF-α and IL-12 are two major mediators of inflammatory responses in mammals able to induce Th1 differentiation necessary for an anti-inflammatory and anti-tumoral response. Upon treatment with Man-PA/**Tn-MIM**, the production and release of high levels of both TNF-α (Fig. 5A) and IL-12 (Fig. 5B) were observed. Glc-PA/**Tn-MIM** was also able to induce the expression of both cytokines, albeit to a lower extent; no effect was observed for **Tn-MIM** itself (Fig. 5). Glc-PA and Man-PA induced interesting levels of IL-12 but only low levels of TNF-α expression. This property allows the correlation of the complete DC differentiation toward a pro-inflammatory phenotype[25] able to induce an antitumor response to the presence of **Tn-MIM**. So globally, these data indicate that (i) Glc-PA and Man-PA have a low stimulatory activity, which can efficiently be increased upon the internalization of **Tn-MIM**; (ii) the stimulatory activity toward a proinflammatory phenotype required to induce an antigen-specific immune response was obtained only when iDCs were treated with Man-PA/**Tn-MIM**.

Internalization of Tn-MIM-integrated nanofibers

iDCs express various surface sugar transporters, including DC-SIGN receptors, which are known to mediate the internalization of mannosylated structures. Accordingly, Man-PA/**Tn-MIM** and Glc-PA/**Tn-MIM**, able to induce DC maturation, were screened in endocytosis assays. iDCs were treated (24 h) with the fluorescent glycopeptide nanofibers Man-PA/**Tn-MIM** BodyPy and Glc-PA/**Tn-MIM** BodyPy (see Fig. 1), harvested, washed, split into two aliquots and counterstained. As shown in Fig. 6A, after 24 h of incubation, the fluorescence can be observed inside the cells. The counterstaining of the nuclei (blue) and the cell surface (anti-HLA-DR red) helps to identify the cells and the cytoplasmatic localization of both fluorescent glycopeptide nanofibers. To further confirm the endocytosis, an aliquot of treated and untreated cells was analyzed by flow cytometry (Fig. 6B).

An increase of cell fluorescence was observed after the treatment with both Man-PA/**Tn-MIM** BodiPy and Glc-PA/**Tn-MIM** BodiPy confirming the cells' internalization of both the **Tn-MIM**-integrated nanofibers.

Immune cell recruitment and activation

To efficiently orchestrate immune responses, DCs shall recruit immune cells at the infected or inflamed site. To evaluate the differentiated DCs' ability to recruit immune cells, chemotaxis assays were performed by using the Boyden chamber method. iDCs plated in the lower compartment of the chamber were treated/untreated (48 h) with the selected compounds, and syngeneic PBMC was added to the upper compartment. After 3 h of co-culture, iDCs were able to recruit CD3+ cells (Fig. S3A). Upon treatment with Man-PA and Glc-PA, a slight but not significant increase in CD3+ cell recruitment was recorded. Only DCs treated with Man-PA/**Tn-MIM** induced a significant increase (+14%) in the recruitment of CD3+ cells (Fig. 7A), highlighting the beneficial effect of **Tn-MIM** inte-

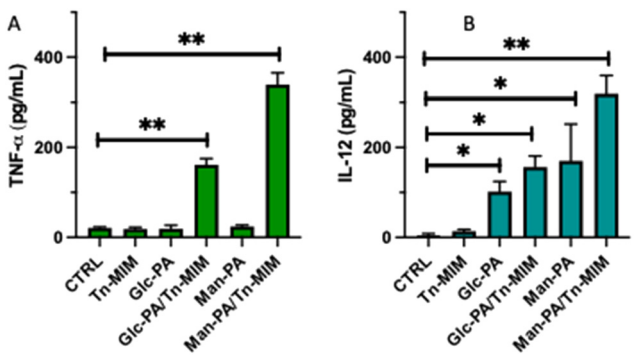

Fig. 5 Cytokines produced by iDCs treated with tested compounds. The media of iDCs treated (48 h) with **Tn-MIM**, Man-PA, Glc-PA, Glc-PA/**Tn-MIM** and Man-PA/**Tn-MIM** (10 μM) were harvested and TNF-α (A) and IL-12 (B) levels were assessed by ELISA. The results represent the mean ± SEM of at least three experiments conducted with iDCs obtained using different donors.

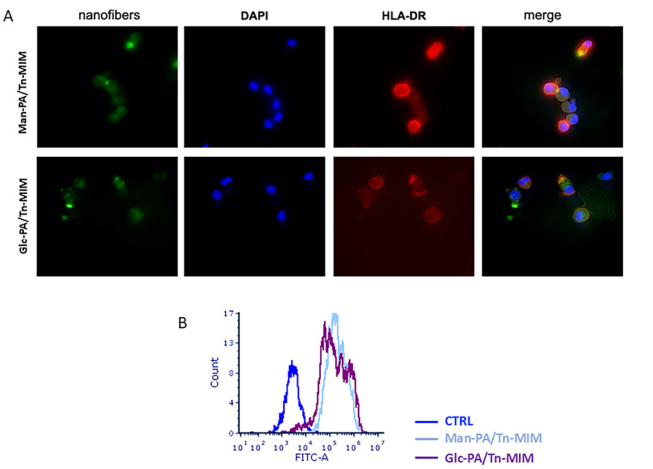

Fig. 6 DCs' internalization of fluorescent **Tn-MIM** integrated nanofibers. iDCs were treated with fluorescent Glc-PA/**Tn-MIM** BodiPy or Man-PA/**Tn-MIM** BodiPy integrated nanofibers (10 μM). (A) After 24 h of treatment, cells were harvested, washed several times to eliminate extracellular bound compounds, and stained with anti HLA-DR, and nuclei were counterstained with DAPI. Nanofibers' localization was analyzed by fluorescent microscopy (nanofibers: green; HLA-DR: red; DAPI: blue). The images are representative of 3 independent experiments giving similar results. (B) After 24 h of treatment, DCs were harvested and washed several times and the fluorescence level (MFI) was analyzed by flow cytometry. The histograms are representative of 3 independent experiments giving similar results.

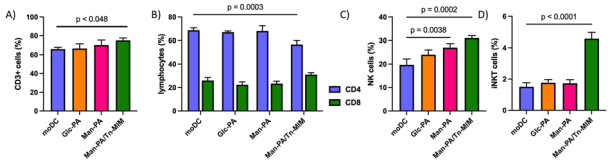

Fig. 7 Glycopeptide nanofibers induce lymphocyte, iNKT and NK cell recruitment. iDCs were plated in the lower compartment of the Boyden chamber and treated (48 h) with Man-PA, Glc-PA or Man-PA/**Tn-MIM** (10 μM) for PBMCs in a chemotaxis assay. The lymphocytes that migrated into the lower chamber were harvested and stained with anti-CD3, anti-CD4, anti-CD8, anti-CD56 and anti-e Vα24/Vβ11 antibodies and the percentages of CD3+, CD4+, CD8+ NK and iNKT cells were analyzed by FACS. (A) Percentage of CD3+ cells. (B) Percentage of CD4+ and CD8+ cells. (C) Percentage of CD56 positive cells. (D) Percentage of iNKT cells. The results represent the mean ± SEM of at least three experiments conducted with iDCs obtained from different donors.

grated in Man-PA. The screening of the CD3 subpopulation showed a slight increase in CD8+ (+28%) cells and a low reduction (−24%) in CD4+ cell recruitment (Fig. 7B and S3B) for DCs treated with Man-PA/**Tn-MIM**.

A similar chemotactic response was recorded for iNKT cells (Fig. 7C and S6A) and NK cells (Fig. 7D and S6B) exposed to DCs treated with Man-PA/**Tn-MIM**.

Finally, the intracellular IFN-γ expression was evaluated to flag recruited immune cells as well as the CD69 activation marker. Man-PA/**Tn-MIM** induced a slight increase in CD69 expression (Fig. 8A) but a significant increase in IFN-γ+ CD4 cells (Fig. 8B).

All together, these data demonstrate that upon treatment with Man-PA/**Tn-MIM**, DCs can recruit immune cells relevant to inducing an antitumor immune response, generating a microenvironment able to induce proinflammatory CD4+ phenotype acquisition.

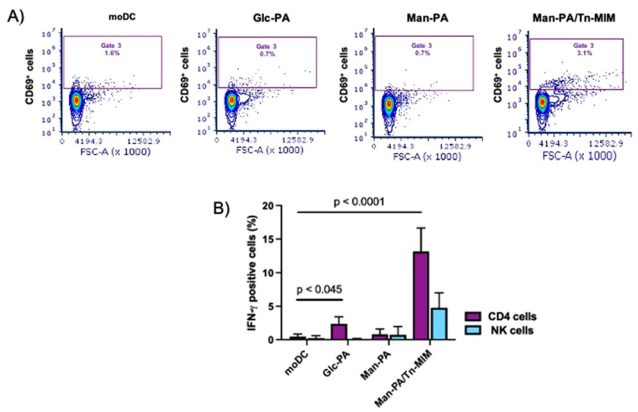

Fig. 8 Activation induced in recruited immune cells. The cells that migrated into the lower compartment of a Boyden chamber were harvested, fixed with 3.7% PFA, permeabilized with 0.1% saponin and stained with anti-CD69 and anti-iFNγ antibodies and the percentages of CD4+/CD69+, CD56+/CD69+, CD56+/IFN-γ+, and CD4/IFN-γ+ cells analyzed by FACS. (A) Representative contour plots of CD69+ cells. (B) Percentage of iFNγ+ NK and CD4 cells. The results represent the mean ± SEM of at least three experiments conducted with iDCs obtained using different donors; *$p \leq 0.05$; **$p \leq 0.01$.

Allostimulation and Th polarization

To further explore the stimulatory properties of the generated DCs, a mixed lymphocyte reaction (MLR) with allogeneic PBMCs was performed. The MLR assay is based on the principle that T cells from one donor will respond and proliferate in the presence of antigen-presenting cells (APCs) from a different donor, caused by a human leukocyte antigen (HLA) mismatch between unrelated donors. The HLA mismatch stimulates the T cells' immune response, inducing their proliferation. The high differentiation and maturation of DCs recorded upon treatment with Man-PA/**Tn-MIM** were reflected in their high allostimulatory activity (Fig. 9 and S7). Man-PA/**Tn-MIM**-treated DCs better stimulated allogeneic PBMC proliferation compared to DCs treated with Man-PA or Glc-PA or with respect to the untreated group (Fig. 9A).

Along with the stimulation of T cell proliferation, a key role of DCs is to shape the T cell effector functions through the polarization of CD4+ T cell differentiation, *via* cytokines secreted by DCs. Allogeneic PBMCs co-cultured with DCs treated with glycopeptide nanofibers were harvested and labelled with anti-CD4, anti-IL-4 and anti-IFN-γ antibodies and the percentages of CD4+/IL-4+ and CD4+/IFN-γ+ cells were analyzed by flow cytometry. As shown in Fig. 9, DCs treated with Man-PA and Glc-PA did not induce any cytokine production. Conversely, upon treatment with Man-PA/**Tn-MIM**, DCs induced an increase in CD4+/IFN-γ+ frequency without affecting CD4+/IL-4+ (Fig. 9B). These data allow us to conclude that Man-PA/**Tn-MIM** mediated the Th1 polarization of CD4 lymphocytes able to sustain a proinflammatory response.

In vitro immune organ-on-chip model assay

To further validate the meaning and properties of glycopeptide nanofibers in immuno-oncological applications, a physiologically relevant test was performed by using an organ-on-chip

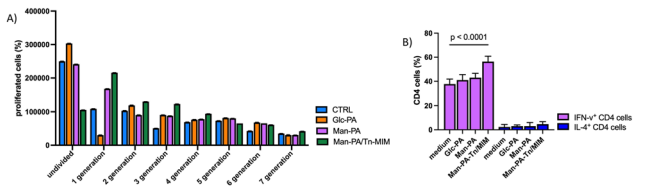

Fig. 9 Allostimulatory ability of DCs treated with glycopeptide nanofibers. DCs treated with Man-PA, Glc-PA or Man-PA/**Tn-MIM** (10 μM) were harvested and used to stimulate CFSE stained allogeneic PBMCs. After 7 days of co-culture, PBMCs were harvested and CFSE dilution was analyzed by flow cytometry. (A) Proliferation induced by PBMCs co-cultured with DCs treated with Man-PA, Glc-PA or Man-PA/**Tn-MIM**. (B) After 2 days of incubation, PBMCs were harvested, fixed with 3.7% PFA, permeabilized with 0.1% saponin and stained with anti-CD4, anti IFN-γ and anti-IL-4 antibodies. After several washes, IFN-γ+/CD4 and IL-4+/CD4 cells were analyzed by flow cytometry. The results represent the mean ± SEM of at least three experiments performed with iDCs obtained from different donors.

platform. Three-dimensional (3D) human breast cancer models were developed by embedding MCF-7 cells in a three-dimensional alginate-based hydrogel, which was then co-cultured under dynamic conditions with CD3+ T cells. These T cells were previously exposed to iDCs treated with either Man-PA/Tn, Man-PA, or Glc-PA nanofibers, or left untreated as controls. The fluid-dynamic co-cultures were carried out using the Single-Flow MIVO® organ-on-chip (React4life, Genoa, Italy), designed to replicate the complexity of a 3D, dynamic tumor microenvironment. In particular, the culture system was specifically engineered to allow *in vivo* like immune cell circulation below the hydrogel-embedded tumor cells (E : T ratio 10 : 1; see the SI), with the tumor model placed in a standard 24-well plate Transwell insert, fitting the MIVO® chamber (see Fig. S8). The device was connected to a pumping system that imposed a physiological fluid flow, driving immune cells through the circulation in a closed circuit, thereby mimicking the circulatory dynamics within the tumor microenvironment. After 18 hours of co-culture, the ability of immune cells to migrate upward (against gravity) in an "extravasation" process, infiltrate the tumor and induce cancer cell apoptosis was assessed. Tumor matrixes were harvested, the hydrogels were dissociated, and the single cell suspension was stained with a fixable cell viability dye (green) and fixed with 3.7% PFA. Fixed cells were counterstained with anti-CD3 and analyzed by FACS. Sample analysis reveals the presence of CD3+ cells in tumor spheroids of all tested conditions, suggesting that lymphocytes can actively migrate toward the tumor.

These results indicate that lymphocytes stimulated with DCs exposed to Man-PA and Man-PA/**Tn-MIM** infiltrate the tumor more than unstimulated and lymphocytes stimulated with DCs exposed to Glc-PA. Moreover, the percentage of infiltrated lymphocytes stimulated with DCs exposed to Man-PA/**Tn-MIM** was significantly increased when compared with the control group (lymphocytes stimulated with DCs exposed to vehicles) (Fig. 10A). To confirm the property of Man-PA/**Tn-MIM** to induce Th1 polarization, we assessed the IFN-γ (*i.e.* the main cytokine produced by Th1 lymphocytes) levels in the chip effluents. As shown in Fig. 10D, stimulated T cells were able to release detectable levels of IFN-γ independently of functionalized peptide nanofiber types. Of note, Man-PA/**Tn-MIM** nanofibers induced a higher IFN-γ amount (+37%) with respect to the other functionalized peptide nanofibers (Fig. 10D). On the basis of fluorescence intensity of tumor cells after Fixable Cell Viability (FITC) dye staining, 3 cell populations have been identified in each plot. According to the test's specificity, the higher fluorescent population corresponds to the dead population, the less fluorescent population to the live population, while the "middle" population is formed by structurally degraded cells that incorporated less dye than dead cells. The latter (about 40% of the total tumor cells, independently of the treatment) were not included in the analysis (see the SI). A significant increase in dead cells was observed in the tumor models co-cultured with circulating lymphocytes stimulated with DCs exposed to Man-PA/**Tn-MIM** with respect to all other groups (Fig. 10B). The statistically significant reduction of live tumor cells in the same samples (Fig. 10C) confirmed the cytotoxicity of lymphocytes stimulated with DCs exposed to Man-PA/**Tn-MIM**.

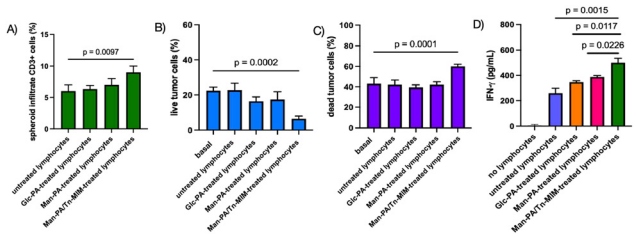

Fig. 10 Extravasation ability of T cells and cytotoxicity induction against tumor cells. T cells previously exposed to iDCs treated with either Glc-PA (Glc-PA lymph), Man-PA (Man-PA lymph) or Man-PA/**Tn-MIM** (Man-PA/**Tn-MIM** lymph) nanofibers or left untreated (untreat. lymph), as controls, were co-cultured, under dynamic conditions, with a 3D tumor model. After 18 h, tumor spheroids were harvested, the hydrogels were dissociated, and the single cell suspension was stained with a fixable cell viability dye (green), fixed with 3.7% PFA, counterstained with an anti-CD3 antibody and analyzed by FACS. (A) Percentage of extravasated CD3+ cells over total spheroid cells. (B) Percentage of live tumor cells. (C) Percentage of dead tumor cells. (D) IFN-γ levels in the chip effluents. The live and dead tumor cells were obtained after the exclusion of the structurally damaged cells (about 40% in each sample; see the SI for details). The results represent the mean ± SEM of at least three experiments.

Experimental

Preparation of self-adjuvating glycopeptide nanofibers Man-PA and Glc-PA

Man-PA and Glc-PA peptide amphiphile molecules were synthesized and purified as described previously.[20] Briefly, MHBA Rink Amide resin was used for the construction of the peptide amphiphiles. Fmoc-protected amino acids were coupled using HBTU and *N*,*N*-diisopropylethylamine (DIEA) in DMF. Fmoc removal was carried out with a piperidine/dimethylformamide (DMF) solution. After the cleavage of the peptides from the resin, deprotection of acid labile protecting groups was performed. Removal of excess TFA was followed by the trituration of the remaining residue, freeze-drying, and deacetylation. Glycopeptides were analyzed by reverse phase HPLC on an Agilent 6530 Accurate-Mass Q-TOF LC/MS equipped with an Agilent 1200 HPLC before and after the deacetylation. The peptide amphiphiles were purified on an Agilent 1200 by using a Zorbax prepHT 300CB-C8 column with a water–acetonitrile (0.1% TFA) gradient.

Cell source

Monocytes differentiated into immature DCs came from healthy volunteer buffy coats. All experiments were performed in accordance with the Guidelines of Italian National Regulation, including EU Regulation 536/2014 and experiments were approved by the ethics committee at Università del Piemonte Orientale. Informed consent was obtained from all healthy volunteers whose blood samples were used to isolate PBMCs.

Conclusions

In this study, mannosylated peptide amphiphile nanofibers were prepared by SSPS, loaded with the MUC-1 Tn antigen mimetic, **Tn-MIM**, and used for targeting the DC-SIGN receptor.

Carriers are generally used to present MUC1 carbohydrate antigens to the immune system[11,22] to boost their potency, while to improve the longevity of the specific immune response adjuvants are necessary. Effective adjuvants like alum, MF59, AS0, CpG, matrix-M and virosome are indeed commonly used in vaccine formulations. Recent studies suggested that to boost specific immune responses, delivery systems that possess intrinsic immunomodulatory activity could be explored. Mannosyl-peptide nanofibers could be included in this group. We have observed that **Tn-MIM**-conjugated mannosyl-peptide nanofibers enter DCs suggesting their ability to deliver antigens into APCs, a necessary step for processing and presenting an antigen. The same ability is possessed by alum and matrix-M adjuvants able to absorb and carry antigens to APCs and facilitate antigen phagocytosis. Moreover, non-conjugated mannosyl peptide nanofibers—and to a greater extent, **Tn-MIM**–conjugated ones—can promote DC differentiation toward a pro-inflammatory phenotype, like the effects of alum, virosomes, matrix-M, and AS adjuvants. Finally, like CpG, **Tn-MIM** conjugated mannosyl-peptide nanofibers were able to induce Th1 switching necessary for complete B cell activation and differentiation towards plasma cells, as documented by the IFN-γ production observed in organ-on-chip experiments.

Altogether, the results herein reported undoubtedly confirmed the potential of Man-PA/**Tn-MIM**, in immuno-oncological applications and will help in the development of a new generation of immunomodulators.

Author contributions

Conceptualization: S. F., M. O. G., A. B. T. and C. N.; investigation: A. S., F. S., G. L., M. E. F. P., M. C. S., and F. C.; supervision: S. S., S. F., and F. M.; original draft writing: S. F. and C. N.; revision: S. S., M. O. G., and A. B. T.; revision & editing: C. N.

Conflicts of interest

Silvia Scaglione and Maria Elisabetta F. Palamà are employed by the company React4life S.p.A.

Note added after first publication

This article replaces the version published on 17th September 2025. Affiliation e and the present address footnote for Mustafa O. Guler have been updated to reflect the institution at which the research was conducted.

Data availability

The data supporting this article have been included as part of the SI. See DOI: **https://doi.org/10.1039/d5bm00304k**.

Acknowledgements

C.N. thanks Fondazione AIRC (Italy), project IG25762 and Banca d'Italia for financial support.

References

1 S. K. Linden, P. Sutton, N. G. Karlsson, V. Korolik and M. A. McGuckin, *Mucosal Immunol.*, 2008, **1**, 183–197.
2 H. Cai, Z. H. Huang, L. Shi, P. Zou, Y. F. Zhao, H. Kunz and Y. M. Li, *Eur. J. Org. Chem.*, 2011, 3685–3689.
3 S. Dziadek, D. Kowalczyk and H. Kunz, *Angew. Chem., Int. Ed.*, 2005, **44**, 7624–7630.
4 J. Zhu, Q. Wan, D. Lee, G. Yang, M. K. Spassova, O. Ouerfelli, G. Ragupathi, P. Damani, P. O. Livingston and S. J. Danishefsky, *J. Am. Chem. Soc.*, 2009, **131**, 9298–9303.
5 D. Zhou, L. Xu, W. Huang and T. Tonn, *Molecules*, 2018, **23**, 1–27.
6 F. Corzana, A. Asín, A. Eguskiza, E. De Tomi, A. Martín-Carnicero, M. P. Martínez-Moral, V. Mangini, F. Papi, C. Bretón, P. Oroz, L. Lagartera, E. Jiménez-Moreno, A. Avenoza, J. H. Busto, C. Nativi, J. L. Asensio, R. Hurtado-Guerrero, J. M. Peregrina, G. Malerba, A. Martínez and R. Fiammengo, *Angew. Chem., Int. Ed.*, 2024, **63**, e202407131.
7 I. Sanz-Martinez, S. Pereira, P. Merino, F. Corzana and R. Hurtado-Guerrero, *Acc. Chem. Res.*, 2023, **56**, 548–560.
8 B. Pulendran, P. S. Arunachalam and D. T. O'Hagan, *Nat. Rev. Drug Discovery*, 2021, **20**, 454–475.
9 S. Akira and K. Takeda, *Nat. Rev. Immunol.*, 2004, **4**, 499–511.
10 Z. H. Huang, L. Shi, J. W. Ma, Z. Y. Sun, H. Cai, Y. X. Chen, Y. F. Zhao and Y. M. Li, *J. Am. Chem. Soc.*, 2012, **134**, 8730–8733.
11 C. Nativi and O. Renaudet, *ACS Med. Chem. Lett.*, 2014, **5**, 1176–1178.
12 B. L. Wilkinson, S. Day, L. R. Malins, V. Apostolopoulos and R. J. Payne, *Angew. Chem., Int. Ed.*, 2011, **50**, 1635–1639.
13 S. Ingale, M. A. Wolfert, J. Gaekwad, T. Buskas and G. J. Boons, *Nat. Chem. Biol.*, 2007, **3**, 663–667.
14 I. Companión, A. Guerreiro, V. Mangini, J. Castro-López, M. Escudero-Casao, A. Avenoza, J. H. Busto, S. Castillón, J. Jiménez-Barbero, J. L. Asensio, G. Jiménez-Osés, O. Boutureira, J. M. Peregrina, R. Hurtado-Guerrero, R. Fiammengo, G. J. L. Bernardes and F. Corzana, *J. Am. Chem. Soc.*, 2019, **141**, 4063–4072.
15 M. B. Demircan, S. Tohumeken, N. Gunduz, M. A. Khalily, T. Tekinay, M. O. Guler and A. B. Tekinay, *Biotechnol. J.*, 2020, **15**, 1–8.
16 J. L. Chen, C. N. Fries, S. J. Berendam, N. S. Rodgers, E. F. Roe, Y. Wu, S. H. Li, R. Jain, B. Watts, J. Eudailey,

R. Barfield, C. Chan, M. A. Moody, K. O. Saunders, J. Pollara, S. R. Permar, J. H. Collier and G. G. Fouda, *Sci. Adv.*, 2022, **8**, 1–15.

17 H. A. F. M. Hassan, M. Haider and S. A. Fahmy, *Mater. Adv.*, 2024, **5**, 4112–4130.

18 J. B. Matson and S. I. Stupp, *Chem. Commun.*, 2012, **48**, 26–33.

19 D. Mumcuoglu, M. Sardan Ekiz, G. Gunay, T. Tekinay, A. B. Tekinay and M. O. Guler, *ACS Appl. Mater. Interfaces*, 2016, **8**, 11280–11287.

20 G. Gunay, M. Sardan Ekiz, X. Ferhati, B. Richichi, C. Nativi, A. B. Tekinay and M. O. Guler, *ACS Appl. Mater. Interfaces*, 2017, **9**, 16035–16042.

21 E. Scheid, P. Major, A. Bergeron, O. J. Finn, R. D. Salter, R. Eady, B. Yassine-Diab, D. Favre, Y. Peretz, C. Landry, S. Hotte, S. D. Mukherjee, G. A. Dekaban, C. Fink, P. J. Foster, J. Gaudet, J. Gariepy, R. P. Sekaly, L. Lacombe, Y. Fradet and R. Foley, *Cancer Immunol. Res.*, 2016, **4**, 881–892.

22 A. Amedei, F. Asadzadeh, F. Papi, M. G. Vannucchi, V. Ferrucci, I. A. Bermejo, M. Fragai, C. V. De Almeida, L. Cerofolini, S. Giuntini, M. Bombaci, E. Pesce, E. Niccolai, F. Natali, E. Guarini, F. Gabel, C. Traini, S. Catarinicchia, F. Ricci, L. Orzalesi, F. Berti, F. Corzana, M. Zollo, R. Grifantini and C. Nativi, *iScience*, 2020, **23**, 101250.

23 R. Mammadov, G. Cinar, N. Gunduz, M. Goktas, H. Kayhan, S. Tohumeken, A. E. Topal, I. Orujalipoor, T. Delibasi, A. Dana, S. Ide, A. B. Tekinay and M. O. Guler, *Sci. Rep.*, 2015, **5**, 1–15.

24 E. van Liempt, C. M. C. Bank, P. Mehta, J. J. García-Vallejo, Z. S. Kawar, R. Geyer, R. A. Alvarez, R. D. Cummings, Y. van Kooyk and I. van Die, *FEBS Lett.*, 2006, **580**, 6123–6131.

25 X. Ma, *Microbes Infect.*, 2001, **3**, 121–129.